




## CO-MODIFICATION OF BENTONITE BY CTAB AND SILANE AND ITS PERFORMANCE IN OIL-BASED DRILLING MUD

MIAO GUO, GUANGBIN YANG\* , SHENGMAO ZHANG, YUJUAN ZHANG, CHUANPING GAO, CHUNLI ZHANG, AND PINGYU ZHANG\*

<sup>1</sup>Engineering Research Center for Nanomaterials, Henan University, Kaifeng 475004 Henan, China

**Abstract**—The stability, dispersion, and rheological properties of clay suspensions are important in the process of drilling. Organic clays were obtained traditionally by cation exchange, which is thermally unstable due to weak electrostatic interaction between the cationic surfactant and clay minerals. The purpose of the present study was to yield a stable and well dispersed organic bentonite (OBent) as a rheological additive for oil-based drilling mud. The co-modified method was used to modify bentonite by a cationic surfactant (cetyltrimethylammonium bromide: CTAB) and a silane coupling agent (hexadecyltrimethoxysilane: HDTMS). Firstly, the basal spacing of bentonite was enlarged by intercalation of CTAB, and the thermal stability of bentonite was improved by covalent bonds of HDTMS onto the bentonite platelets. The as-prepared OBent was characterized by infrared analysis, X-ray diffraction analysis, thermogravimetric analysis, and scanning electron microscopy. The hydrophobicity, solubility, viscosity, and tribological performance of the OBent were also recorded. The test results showed that the hydrophobicity of the co-modified bentonite was improved significantly, and was greater than that of bentonite modified with single surfactant CTAB or HDTMS. The bentonite modified by the surfactant together with the silane coupling agent had stable rheology and a lower coefficient of friction than the single surfactant-modified bentonite because more HDTMS entered into the interlayer spaces and formed chemical bonds at the inner surface of platelets.

**Keywords**—Bentonite · Co-modification · Oil-based mud · Rheology · Stability

### INTRODUCTION

Drilling fluids play an essential role in drilling engineering and can determine the success or failure of a drilling project. The main functions of drilling fluid are to: (1) remove the cuttings from the drill bit and transport them to the floor; (2) lubricate and cool the drill bit and reduce friction; (3) keep the wellbore stable; (4) form a dense filter cake; and (5) bring information back to surface level, etc. (Huskić et al. 2013). Drilling fluids are divided into water-based and oil-based. Currently, water-based drilling fluids are most commonly used in the drilling industry, because they are relatively environmentally friendly and cheap (Caenn and Chillingar 1996; Meng et al. 2012; Shen et al. 2019). Typically, they are used at low temperature and low pressure. Water-based drilling fluids, however, are limited by their interference with the flow of gas and oil through porous rock and their ability to dissolve salts. Oil-based drilling fluids are used widely in high-temperature and high-pressure wells, such as deep or ultra-deep wells, large-angle wells, etc., because of their lubricating properties, shale inhibition performance, and wellbore stability (Caenn and Chillingar 1996; Meng et al. 2012).

In recent years, organic clays have been used widely in nano-composites (El Gaidoumi et al. 2018, 2019c), catalyst carriers (El Gaidoumi et al. 2019a, 2019b), waste treatment (Battas et al. 2019; Mustapha et al. 2020), and environmental remediation (Awad et al. 2019; Shen and Gao 2019); this is because they are low cost, have significant adsorption efficiency, show good recyclability, and because of their good ecological compatibility. Organic clay is also an indispensable part of

drilling fluid, and is one of the important factors that affects the rheological properties of drilling fluids. Bentonite (Bent) is a non-metallic mineral with montmorillonite (Mnt) as the main mineral component. Mnt is a layered aluminosilicate with a two-dimensional nanosheet structure. Its crystal structure is a monoclinic 2:1 layered silicate formed by two Si–O tetrahedral sheets encompassing an Al–O (OH) or Mg–O (OH) octahedral sheet. Natural Mnt is hydrophilic. Due to cations such as Na<sup>+</sup> and Ca<sup>2+</sup> between Mnt layers, water molecules enter the interlayer space of the clay, which leads to easy hydration and expansion of Mnt (Sinha Ray and Okamoto 2003; Erdem et al. 2010; Kaufhold and Dohrmann, 2013; Chen et al. 2018). In order to obtain hydrophobic Mnt, it must be modified. Intercalation treatment and surface grafting agents were used to prepare organoclay (de Paiva et al. 2008; Bergaya and Lagaly 2001; He et al. 2014). Surfactants, such as alkyl quaternary ammonium salts, have been used widely in industry. The specific method involves, firstly, organic treatment of Mnt, i.e. ion exchange, and exchange of the cations in the Mnt interlayer. Organic surfactants increased the interlayer spacing of the Mnt layer, and promoted the intercalation of other organic surfactants. Common surfactants such as alkyl quaternary ammonium could increase the interlayer spacing and hydrophobicity of the clays (Bujdák 2015; Zhuang et al. 2015; Fu et al. 2016; Sun et al. 2016; Gamba et al. 2017). Although cationic surfactants enter the clay interlayer easily, cationic surfactants such as quaternary ammonium salts are linked by relatively weak electrostatic forces or van der Waals forces; they would decompose at ~150°C, resulting in poor temperature resistance, therefore. The rheological properties of drilling fluids were difficult to control at high temperature (Xie et al. 2001; He et al. 2005; Xi et al. 2007). The use of organosilanes to modify bentonite improved the thermal

\* E-mail address of corresponding author: yang0378@henu.edu.cn

DOI: 10.1007/s42860-020-00093-7

© The Clay Minerals Society 2021

stability and hydrophobic properties (Zhu et al. 2007). The silylation reaction between organosilanes and hydroxyl groups on the surface of bentonite was grafted covalently and provided a stable chemical linkage between organosilane and bentonite (Waddell et al. 1981; Hunnicutt and Harris 1986; Impens et al. 1999). Mnt was modified with octadecyltrimethoxysilane (Song et al. 2001), but the silane coupling agent was grafted mainly on the edge of the Mnt platelets, and the spacing of the Mnt platelets before and after modification did not change.

Studies have shown that the intercalation of cationic surfactants was related to the length of the alkyl chain (Yang et al. 1999; Zhuang et al. 2017a, 2019). Molecules with longer alkyl chains were less likely to intercalate. Molecules with shorter alkyl chains are less soluble in oil. In order to produce a stable and well dispersed organic bentonite (OBent) as a rheological additive for oil-based drilling fluids, bentonite was co-modified by cationic surfactant of cetyltrimethoxyammonium bromide (CTAB) and silane of hexadecyltrimethoxysilane (HDTMS). The CTAB was used to enlarge the basal spacing ( $d_{001}$ ) of the montmorillonite in the bentonite. The HDTMS was used to improve thermal stability and dispersion of bentonite by a condensation reaction between the silanol groups of bentonite surfaces and hydroxyl groups of hydrolyzed HDTMS. Furthermore, in order to control the cost suitability of the proposed OBent, the total amount of surfactant was kept constant, adjusting the dosage ratio of CTAB and HDTMS to achieve optimization. The effects of the ratio of CTAB and HDTMS and the types of modifiers on the oil solubility and thermal stability of OBent were investigated in the present study.

## MATERIALS AND METHODS

### Materials

Bentonite was supplied by China National Petroleum Corporation (Bohai Drilling Engineering Company Limited, Tianjin, China). The CTAB was obtained from Tianjin Kemiu Chemical Reagent Co., Ltd., (Tianjin, China). The HDTMS was provided by Chenguang Chemical Co., Ltd. (Qufu, Shandong, China). Hydrochloric acid and ethanol were both of analytical grade and used as received. The white oil (No. 5) was purchased from Hubei Borun Chemical Co. Ltd (Jingmen, Hubei, China). The experiment was carried out in distilled water.

### Preparation of OBent

OBent was prepared as follows: 40 g of bentonite passed through a 200 mesh sieve was put into a 500 mL, three-necked flask with 150 mL distilled water. After heating to 80°C, a specific amount of CTAB was added (1.5, 1.0, 0.75, or 0.5 g; the amount of CTAB added for each group of experiments is shown in Table 1), and kept for 2 h. The reaction solution was adjusted to pH 4 with 1 M HCl. Subsequently, a different dosage of HDTMS with 50 mL ethanol was added, and reacted for a further 16 h. Finally, the samples were obtained by centrifuging, washing, drying, milling by hand in an agate mortar, and passing a 200 mesh sieve. The corresponding abbreviation of samples and dosages of CTAB and HDTMS in each group of experiments are shown in Table 1.

**Table 1.** The dosages of CTAB and HDTMS and corresponding abbreviated names of the samples in each group of experiments

| Sample name                   | HDTMS (g) | CTAB (g) |
|-------------------------------|-----------|----------|
| CTAB-Mt                       | 0         | 1.5      |
| HDTMS (0.5)-CTAB (1)-Bent     | 0.5       | 1        |
| HDTMS (0.75)-CTAB (0.75)-Bent | 0.75      | 0.75     |
| HDTMS (1)-CTAB (0.5)-Bent     | 1         | 0.5      |
| HDTMS-Bent                    | 1.5       | 0        |

### Preparation of OBent/Oil Fluids

12 g of OBent and 400 mL of 5# white oil were blended in a high-speed mixer capable of stepless, variable frequency adjustment (Qingdao Tongchun Oil Instrument Co. Ltd., Qingdao, Shandong, China) at 10000 rpm for 20 min, using a  $\varnothing 26$  mm circular rotor blade with ripple fixed on a stirring column, and relative centrifugal force of  $\sim 1450\times g$ . Then the solution was aged at temperatures of 150 and 180°C in a rotary oven for 16 h.

### Characterization

Infrared analysis was conducted using a VERTEX 70 Fourier-transform infrared (FTIR) spectrometer (Bruker, Karlsruhe, Germany). X-ray diffraction (XRD) analysis was carried out using a D8 Advance X-ray power diffractometer (Bruker, Karlsruhe, Germany), running under  $\text{CuK}\alpha$  radiation, 40 kV, 40 mA, and a scan speed of 0.05 s per step (step size:  $0.02^\circ 2\theta$ ). The XRD patterns were collected from  $1$  to  $25^\circ 2\theta$ . Thermogravimetry (TG) was performed using a TAQ600 synchronous thermal analyzer (TA Instruments, New Castle, Delaware, USA) in air from 25 to 800°C with a heating rate of 10°C/min. The derivative thermogravimetric (DTG) curve was used to analyze accurately the mass loss at various temperatures. Images were obtained using a scanning electron microscope (SEM, Carl Zeiss, Jena, Thuringia, Germany) with an operating voltage of 1 kV. Prior to the SEM test, the samples were first coated with a layer of gold using a (Au) using a 108 Auto Sputter Coater (Ted Pella, Inc. Redding, California, USA) operating at 2500 Pa, 30 mA current, and for 120 s. The contact angle was measured on a DSA100S fully automatic folding optical path contact-angle measuring instrument (Kruss, Hamburg, Germany) with distilled water. The samples were pelletized on a YPJ-40T Tableting Machine (Nobadi Material Technology Co., Ltd. Zhengzhou, Henan, China) at load 15 N for 15 min and polished with 800 mesh sandpaper before contact-angle testing. The gel volume was measured by pouring 100 mL of aging solution into a graduated cylinder with a stopper and standing for 24 h. Rheological properties (such as apparent viscosity (AV) and plastic viscosity (PV)) of oil-based drilling muds were measured using a ZNN-D6 six-speed rotary viscometer (Hengtai Da Mechanical and Electrical Equipment Co. Ltd, Qingdao, Shandong, China) at 25°C. AV =  $1/2 \Phi 600$  ( $\Phi 600$  is a dial reading of 600 rpm, which corresponds to a shear rate of  $1021.8 \text{ s}^{-1}$ ). PV =  $\Phi 600 - \Phi 300$  and YP =  $1/2 (\Phi 300 - \text{PV})$ . The tribological properties of the oil-based drilling muds were

determined using a UMT-2 micro-friction and wear tester (Bruker, Karlsruhe, Germany) in reciprocating mode. Silicon wafer and silicon nitride ball with a diameter of 4 mm were selected as friction pairs. The friction was measured at a load of 8 N and a frequency of 2 Hz for 15 min. The Bruker Contour GT-K three-dimensional topography (Bruker, Karlsruhe, Germany) was employed to observe morphology and evaluate the rate of wear of the wear scar on the friction pairs.

## RESULTS AND DISCUSSION

### XRD of OBent Powders

The basal spacing of the unmodified bentonite was 1.42 nm, and the spacing of the bentonite platelets modified with CTAB increased to 1.73 nm (Fig. 1), indicating that CTAB entered the interlayer space of bentonite, and as a result, the interlayer spacing was enlarged. In addition, the basal spacing of OBent was 1.43 nm, 1.42 nm, and 1.41 nm when HDTMS was modified on the surface of CTAB-Bent (Fig. 1), smaller than CTAB-Bent, indicating that the addition sequence of CTAB and HDTMS had an influence on the intercalation reaction. The reason may be that the occurrence of side reactions between HDTMS molecules on the bentonite led to bridging and interlocking of the platelets, resulted in a decrease of the  $d_{001}$  value (Asgari et al. 2017). The  $d_{001}$  value of bentonite modified with HDTMS alone was 1.49 nm (Fig. 1), and the amount of interlayer HDTMS was reduced because no enlargement in basal spacing occurred without intercalation of the cationic surfactant. Most HDTMS was adsorbed on the surface and edge of the bentonite platelets, and the hydrolytic condensation reaction between the layers was reduced. Therefore, the  $d$  value of bentonite modified by HDTMS alone was relatively large compared with the  $d$  value of HDTMS (x)-CTAB (y)-Bent. The observation that HDTMS entered between the bentonite layers was verified further by contact angle and TGA.

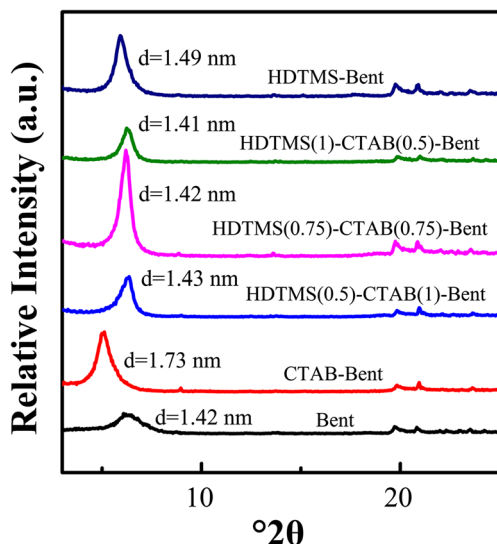


Fig. 1. XRD patterns of bentonite and OBent

The total amount of surfactant remained unchanged, and the ratio of HDTMS to CTAB was adjusted. The mass ratio of HDTMS to CTAB is different in HDTMS (0.5)-CTAB (1)-Bent, HDTMS (0.75)-CTAB (0.75)-Bent, and HDTMS (1)-CTAB (0.5)-Bent; the basal spacings of these three samples were 1.43, 1.4, and 1.41 nm, respectively. CTAB first entered the interlayer of bentonite by ion exchange to enlarge the basal spacing of the bentonite platelets, which promoted HDTMS to enter into the interlayer of bentonite and form covalent bonds between the hydrolysable constituents of HDTMS and the hydroxyl groups of bentonite. As the amount of CTAB was decreased and the amount of HDTMS increased, the  $d$  value of organic bentonite decreased slightly. An increase in the amount of silane coupling agent entering the interlayer of bentonite, and the organic content between the platelets also increased. Side reactions of HDTMS molecules in the system gave rise to bridging and interlocking of the platelets, thereby narrowing the layer spacing of bentonite (Pavlidou and Papaspyrides 2008; Asgari et al. 2017).

### FTIR Spectra

The infrared spectra of bentonite and OBent (Fig. 2) showed that the peak at 400–900  $\text{cm}^{-1}$  was the bending vibration peak of Si–O and Al–O, and the Si–O–Si stretching vibration was located at 1042  $\text{cm}^{-1}$ , which was the characteristic peak of bentonite. Compared with the FTIR spectra of bentonite and CTAB, those of CTAB-Bent showed asymmetric and symmetric stretching vibrations of C–H at 2928 and 2851  $\text{cm}^{-1}$ , and the characteristic absorption peak of the ammonium group was at 1475  $\text{cm}^{-1}$ , showing that the cation CTAB had carried out ion exchange with the cation of bentonite. In contrast to the FTIR spectra for Bent, those for HDTMS-Bent exhibited methyl asymmetric stretching vibration and methylene symmetric stretching vibrations at 2922 and 2851  $\text{cm}^{-1}$ , indicating that silane entered the bentonite layer or was modified on the surface of bentonite.

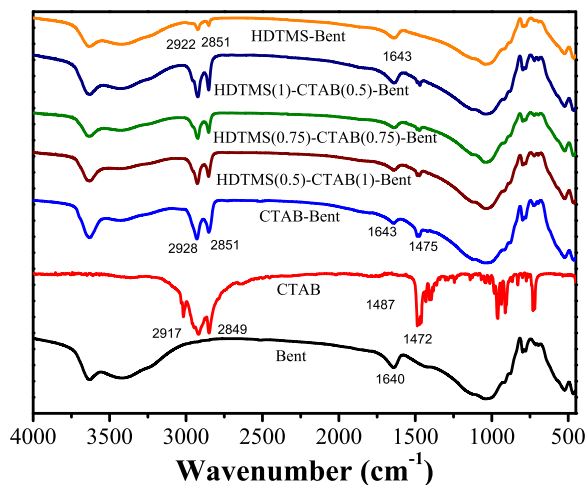


Fig. 2. FTIR spectra of CTAB, bentonite, and OBent

### Thermal Analysis

Bentonite exhibited two steps in terms of weight loss (Fig. 3a,b). The weight loss of bentonite was less than that of OBent. Weight loss below 200°C was due to adsorbed water and free water between bentonite layers (Shanmugaraj et al. 2006; Piscitelli et al. 2010). Because sodium bentonite is hydrophilic, its layers and surfaces are usually covered with a water film. Another weight loss between 600 and 700°C was caused mainly by dehydroxylation of aluminosilicate groups existing in the bentonite structure (Asgari and Sundararaj 2018b). CTAB-Bent demonstrated two obvious weight losses above 200°C. 3.7% of weight loss was measured in the TG curve between 200 and 320°C, which was attributed to the degradation weight of cationic surfactant adsorbed on the bentonite surface. Between 320 and 460°C, a weight loss of ~8.8% was assigned to degradation of cationic surfactant between bentonite layers.

As for HDTMS (0.5)-CTAB (1)-Bent, four weight-loss stages were observed in the TG curve. The first stage between 250 and 390°C was ascribed to decomposition of cationic surfactant physically adsorbed on the bentonite surface. The second stage at 390–460°C was assigned to dehydration of cationic surfactant in the interlayer. The third stage was from 460 to 500°C, which was the degradation of HDTMS chemisorption on interlayers and layer edges of bentonite (Asgari et al. 2017; Asgari and Sundararaj 2018a). The fourth stage, between 550 and 700°C, was due to dehydroxylation. The weight losses of the four stages were ~4.4%, 2.1%, 1.9%, and 3.6%, respectively. The weight loss of dehydroxylation disappeared as the amount of HDTMS increased in the HDTMS(x)-CTAB(y)-Bent ( $x > 0.5$ ), because of the consumption of hydroxyl groups by the silylation reaction (Asgari and Sundararaj 2018b). HDTMS (0.75)-CTAB (0.75)-Bent showed two distinct weight-loss events. The weight loss of ~10.7% between 300 and 460°C was due to the decomposition of CTAB intercalated in the bentonite. A 5.3% weight loss was observed from 460 to 600°C, which was caused predominantly by the decomposition of HDTMS adsorbed on the clay edge and interlayer surfaces. In addition, no weight loss was found between 200 and 300°C, indicating no excess adsorption of HDTMS and cationic surfactants on the bentonite. In the TG curve of

HDTMS -(1)- CTAB (0.5)-Bent, the 7% weight loss at 300–460°C was ascribed to the decomposition of intercalated CTAB. The weight loss which appeared at 460 to 600°C corresponded to the decomposition of HDTMS at the bentonite edge and interlayer. The weight loss increased to 6.5% through the temperature range of 460 to 600°C, because the amount of HDTMS increased in the reaction system.

Similar to the TG curve of bentonite, HDTMS-Bent exhibited obvious weight loss between room temperature and 200°C. At 200–350°C, the thermal weight loss was 0.6% due to physical adsorption of HDTMS. Furthermore, the 4.3% weight loss at 350–600°C was assigned to the thermal degradation of HDTMS chemically grafted on bentonite, less than the amount of HDTMS chemically grafted on HDTMS (1)-CTAB (0.5)-Bent (6.5%) and HDTMS (0.75)-CTAB (0.75)-Bent (5.3%). The reason was that HDTMS could not enter the interlayers of bentonite because the basal spacing had not been enlarged (because there had been no intercalation of cationic surfactant into the bentonite). Furthermore, HDTMS (0.75)-CTAB (0.75)-Bent, HDTMS (1)-CTAB (0.5)-Bent, and HDTMS-Bent displayed no decomposition at 600–700°C. No interlayer water was removed from bentonite when HDTMS was introduced into CTAB-Bent, indicating that the condensation reaction between the hydroxyl groups of the bentonite platelets and silane had taken place. This proved also the intercalation of organosilane. In addition, the degradation temperature of OBent co-modified by HDTMS and CTAB increased, indicating that the thermal stability of bentonite improved when surfactant and bentonite were connected by covalent bonding (Geyer et al. 2014; Asgari et al. 2017; Asgari and Sundararaj 2018a, 2018b; Raji et al. 2018).

### SEM Morphology

The SEM images of the raw bentonite structure showed that the packing was tight, and the size of bentonite flakes was large with many layers (Fig. 4a). The morphology of CTAB-Bent was no different from that of raw bentonite and was only slightly affected by the surfactant CTAB in the interlayer (Fig. 4b). The co-modified bentonite became thin lamellae and exhibited various degrees of curling, the lamellae became

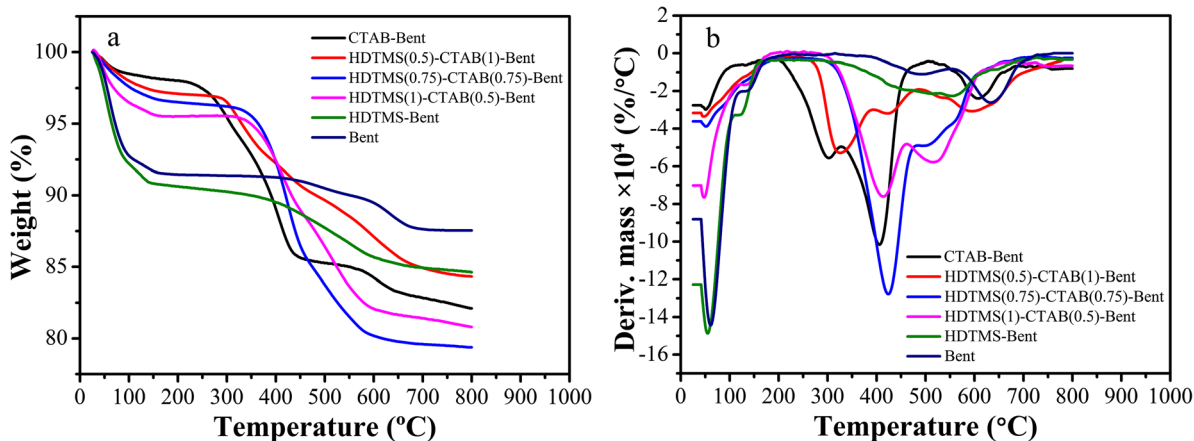
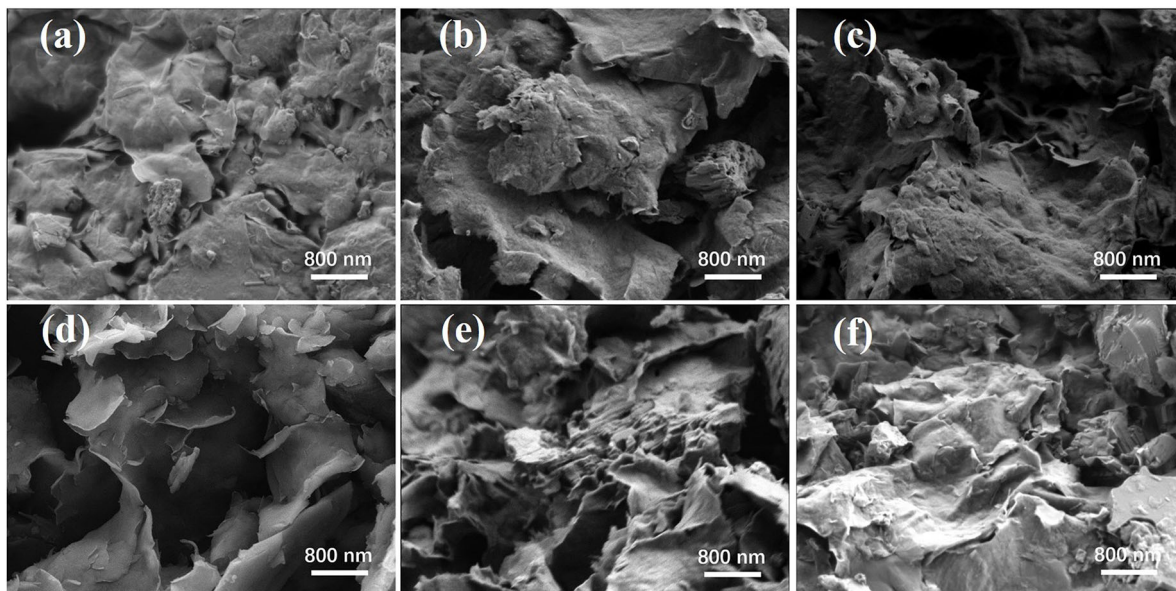


Fig. 3. a TGA and b corresponding DTG curves of bentonite and OBent





**Fig. 4.** SEM images of bentonite and OBent: **a** Bent, **b** CTAB-Bent, **c** HDTMS (0.5)-CTAB (1)-Bent, **d** HDTMS (0.75)-CTAB (0.75)-Bent, **e** HDTMS (1)-CTAB (0.5)-Bent, and **f** HDTMS-Bent

loose and easily suspended. In particular, the morphology of HDTMS (0.5)-CTAB (1)-Bent remained as an unresolved stack of flakes (Fig. 4c). With the increase in surfactant HDTMS, more bentonite lamellae emerged and the edges of lamellae exhibited obvious curling (Fig. 4d,e). The intercalation of the two surfactants into the interlayer space of bentonite did not lead to a great increase in the basal spacing, but resulted in a decrease in the attraction between adjacent lamellae. Finally, looser, thinner lamellae and a number of well-separated flakes emerged.

#### Contact-Angle Test

The contact-angle test is used widely to study the surface and interface properties of OBent. Bentonite was superhydrophilic, the contact angle was so small that it could barely be measured (Fig. 5). The hydrophobicity of the bentonite improved when the surfactants were introduced into the bentonite, 52.4° for CTAB-Bent, 111.5° for HDTMS (0.5)-CTAB (1)-Bent, 142.8° for HDTMS (0.75)-CTAB (0.75)-Bent, 150.4° for HDTMS (1)-CTAB (0.5)-Bent, and 19.2° for HDTMS-Bent (Fig. 5). The contact angle increased with the addition of HDTMS in CTAB-Bent; the hydrophobic performance increased as the amount of HDTMS increased. This result was consistent with the results of TG and XRD. However, the hydrophobicity of HDTMS-Bent was not an obvious change. Bentonite without intercalation by CTAB was modified directly by HDTMS. As a result, the *d* value did not increase and less HDTMS was modified and did not effectively intercalate into the interlayer space of the bentonite.

#### Gel Volume

The compatibility was characterized by gel volumes of drilling muds aged at 34, 150, and 180°C (Fig. 6). 3 g of

bentonite or OBent was dissolved ultrasonically in 100 mL of white oil on an SB-5200DTD Ultrasonic Cleaner (Ningbo Scieniz Biological Technology Co., Ltd. Ningbo, Zhejiang, China) with the power of 200 W, 100 Hz, 30 min. After 24 h at a temperature of 34°C, HDTMS (x)-CTAB (y)-Bent (x,y=0.5,0.75,1.0) presented a greater gel volume. After aging at 150°C, and resting for 24 h at room temperature, HDTMS (x)-CTAB (y)-Bent and HDTMS-Bent still displayed large gel volumes, indicating that the modifier molecules entered the bentonite layers and increased the oil solubility of the bentonite after a certain high-temperature treatment. After aging at 180°C and keeping for 5 h at room temperature, HDTMS (1)-CTAB (0.5)-Bent exhibited the largest gel volume among the six samples tested, then after standing for a further 24 h, all

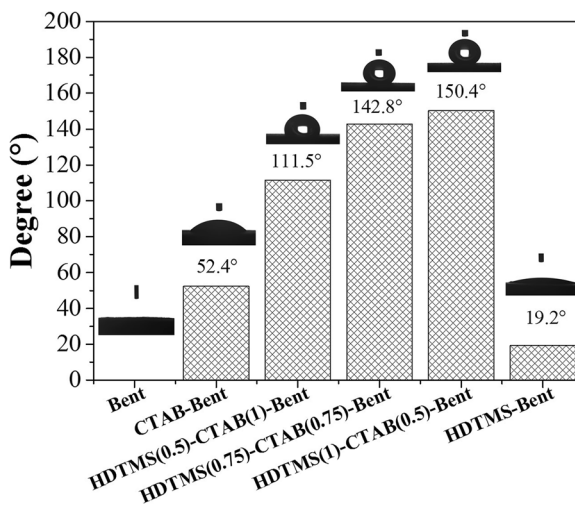


**Fig. 5.** Contact-angle measurement of bentonite and OBent

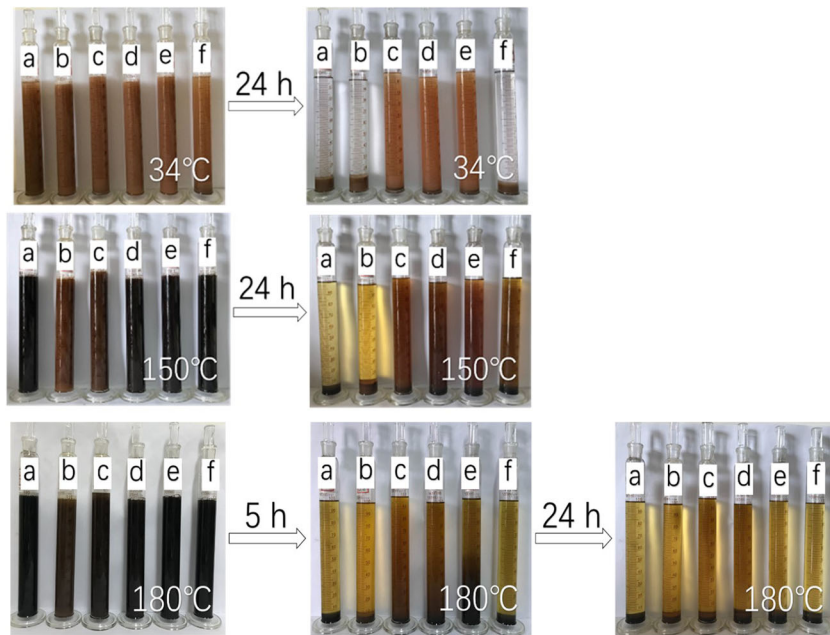


**Fig. 6.** Gel-volumes of Bent and OBent aged at various temperatures, **a** Bent, **b** CTAB-Bent, **c** HDTMS (0.5)-CTAB (1)- Bent, **d** HDTMS (0.75)-CTAB (0.75)-Bent, **e** HDTMS (1)-CTAB (0.5)- Bent, and **f** HDTMS-Bent

samples had a gel volume of almost 0, proving that the modifier HDTMS, to some extent, increased the oil solubility and high-temperature resistance of bentonite. The exchangeable

sites of the CTAB-Bent lamellae were occupied by CTAB, and the alkyl chains are entangled with each other, which created a physical adsorption on the bentonite. The bentonite

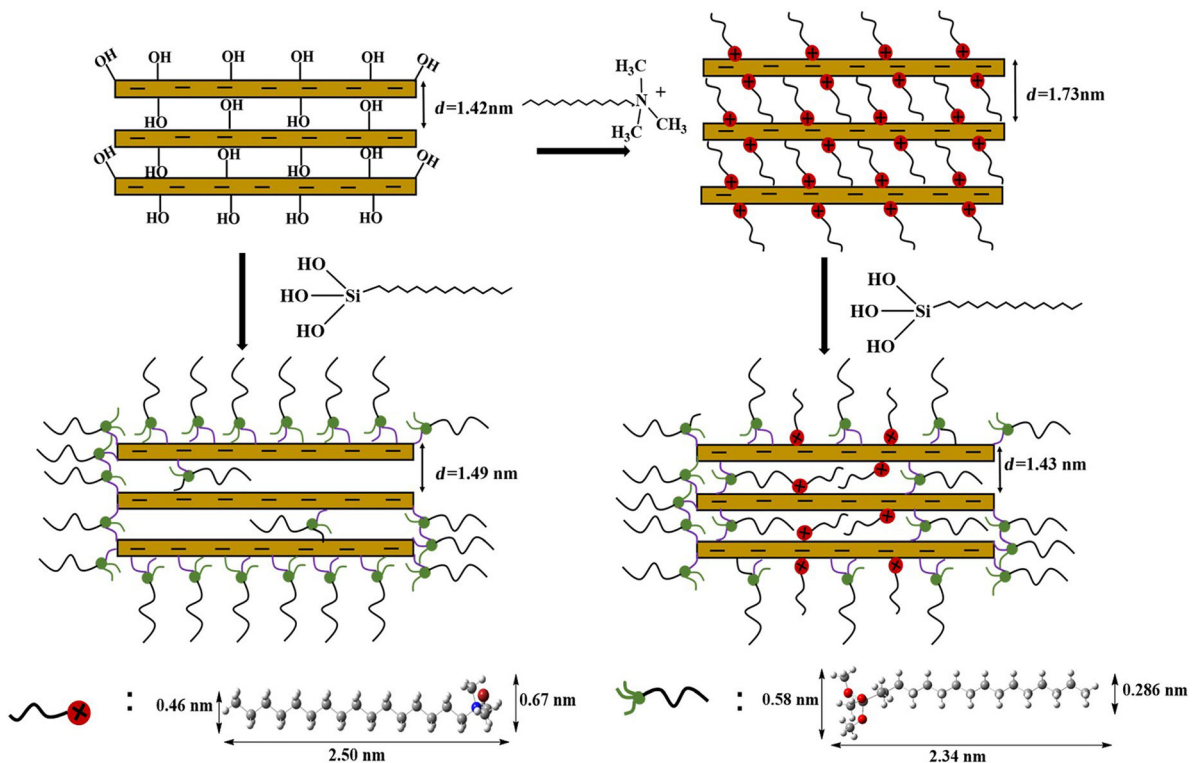


**Fig. 7.** Schematic diagram of the reaction mechanism between the clay layers and modifiers

lamellae were connected to each other and the network structure was established, then a gel was formed. The thermal stability of the gel was poor, however, because it was formed by ionic bonding between CTAB and bentonite. In HDTMS (x)-CTAB (y)-Bent, the bentonite interlayer was occupied by CTAB and HDTMS, and the surfaces of bentonite lamellae were all modified by HDTMS. On one hand, the bentonite was modified by double surfactants which improved the oil solubility of the gel. On the other hand, the covalent bond between HDTMS and bentonite improved the thermal stability of the gel. Therefore, the gel volume increased with increase in HDTMS dosage with HDTMS (1)-CTAB (0.5)-Bent demonstrating the largest gel volume. This result was consistent with the research results that the combination of HDTMS and CTAB led to better compatibility between oil and OBent (Zhuang et al. 2016). Only when HDTMS was modified on bentonite could the oil solubility not be improved obviously due to the small amount of HDTMS modified on the bentonite.

#### Interactions of Surfactants and Bentonite

Based on the experimental data and analysis above, the reaction mechanism models between bentonite layers and modifiers was proposed (Fig. 7). When CTAB was used to modify bentonite, a large amount of cationic surfactant entered the bentonite interlayer through ion exchange and a small amount of cationic surfactant was adsorbed on the bentonite external surface. The  $d$  value of bentonite increased, therefore, from 1.42 to 1.73 nm. When the coupling agent HDTMS was added to the system, it easily entered the interlayers due to the expanded basal spacing caused by the intercalated CTAB. In addition, more HDTMS could enter the interlayer of bentonite with the increase in HDTMS concentration in the system. At that stage, the  $-OH$  of the bentonite reacted with  $Si-OH$  of HDTMS at the edges or internally. Of course, between bentonite layers, the  $Si-OH$  of HDTMS also reacted with the hydroxyl groups of bentonite. The HDTMS at the edges of the platelets underwent condensation reactions, thus reducing the interlayer distance. The condensation reaction of HDTMS caused shrinkage of the bentonite layer. As a result, the  $d$  value decreased to 1.43 nm. As for HDTMS-Bent, because of the lack of cationic surfactant intercalation, less condensation reaction occurred between bentonite layers, so the interlayer distance had no obvious change compared with the  $d$  value of bentonite.

#### Rheological Properties of OBent in Oil

Viscosity is an important factor reflecting the rheological properties of drilling muds and organic clays are used commonly to increase that viscosity (Zhong and Wang 2003; Minase et al. 2008). The viscosity of drilling muds is not only affected by the properties of organic clay but also by temperature. The PV and AV of bentonite decreased significantly after aging at 150°C (Fig. 8). The PV and AV values of CTAB-Bent and HDTMS-Bent decreased slightly after aging at 150°C, while the PV and AV values of bentonite co-modified by HDTMS and CTAB exhibited a slight increase after aging. The increase in the amount of

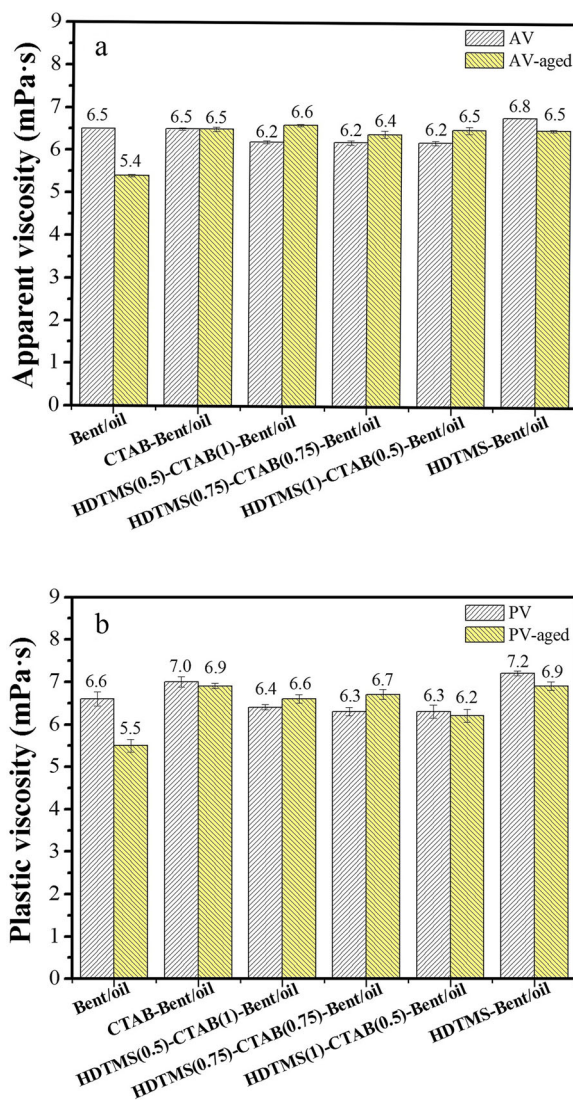
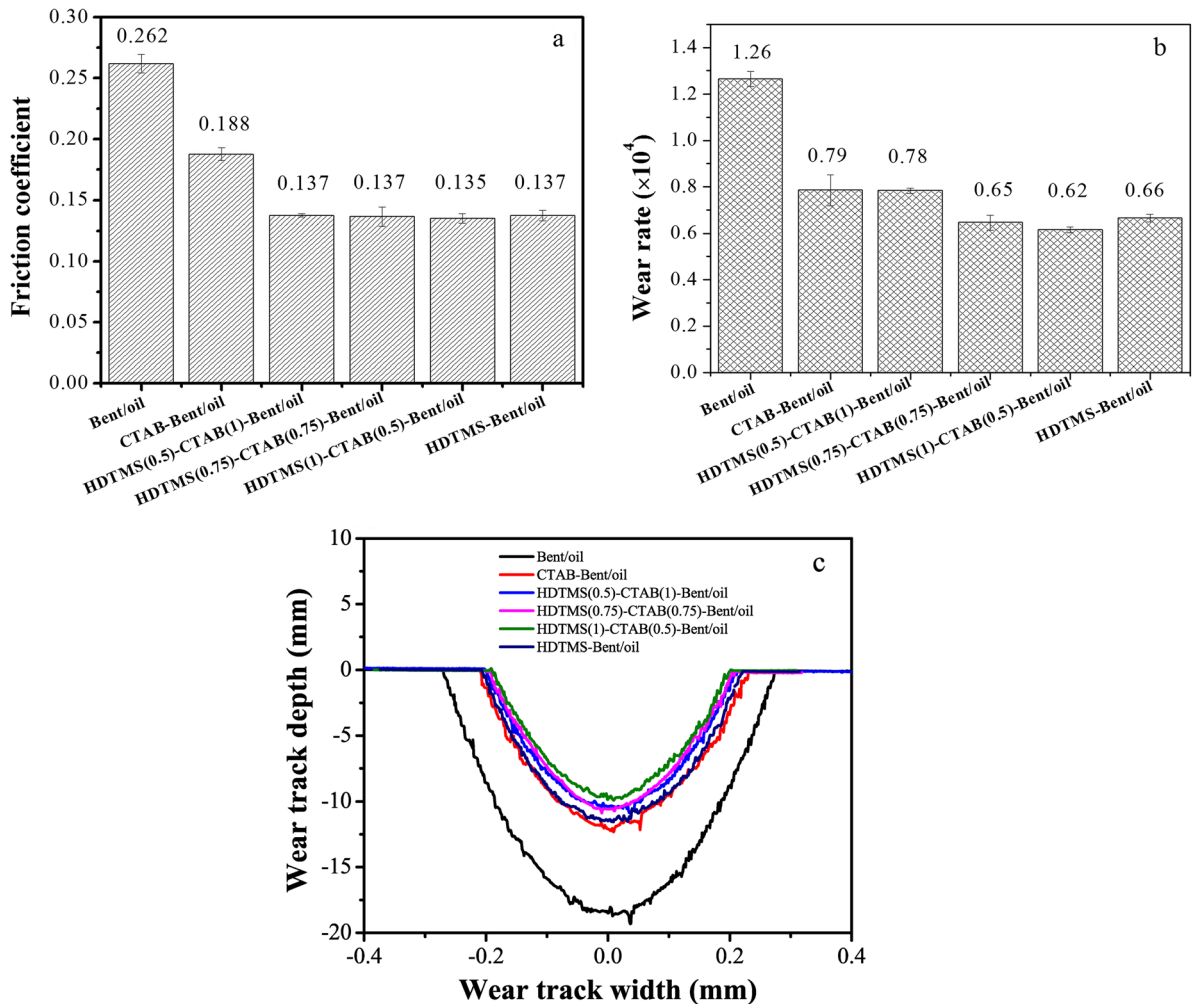


Fig. 8. Rheological properties of OBent/oil fluids before and after aging at 150°C: **a** apparent viscosity and **b** plastic viscosity

HDTMS had no significant effect on the viscosity of the drilling muds. The viscosity of drilling fluid was related not only to the intercompatibility of bentonite and white oil, but also to the microstructure of bentonite in white oil. In Bent/oil, Brownian motion of the bentonite particles intensified after aging at 150°C, and the collision frequency of bentonite particles increased. The ‘house of cards’ structure formed by the ‘edge-to-edge’ and ‘edge-to-face’ of bentonite particles was destroyed and the viscosity decreased, therefore (van Olphen, 1964). As for CTAB-Bent/oil, on one hand, the surfactant on CTAB-Bent was exfoliated as the temperature of CTAB-Bent/oil increased. On the other hand, the white oil molecules entered the interlayer space to swell the organic bentonite which increased the space between bentonite layers and the degree of the organic chain of cationic surfactants (Zhuang et al. 2016, 2017b). The AV





**Fig. 9.** Tribological test results: **a** coefficient of friction diagram, **b** wear rate diagram, and **c** two-dimensional wear diagram of bentonite and OBent in white oil

and PV of CTAB-Bent/oil remained almost unchanged or decreased slightly. HDTMS (x)-CTAB (y)-Bent reported a smaller basal spacing than CTAB-Bent, so fewer oil molecules entered the bentonite layer, resulting in a lower viscosity than CTAB-Bent. After aging at 150°C, mutual motion between bentonite and the organic alkyl chain strengthened and the chain stretched, which increased the connection between the bentonite units. Like CTAB-Bent, oil molecules entered the bentonite layer of HDTMS-Bent easily, because the interlayer distance of HDTMS-Bent was larger than that of HDTMS (x)-CTAB (y)-Bent. After aging at 150°C, less modifier was retained on the clay and the viscosity decreased slightly after aging. Therefore, the optimal viscosity was affected by multiple factors, such as temperature, the interlayer distance, and the type of modifier. In general, HDTMS (x)-CTAB (y)-Bent exhibited high-temperature resistance and better rheological properties due to the interaction of CTAB and HDTMS (Zhuang et al. 2016) and CTAB promoted the adsorption of HDTMS on

bentonite. The increase in organic matter content of bentonite strengthened the entanglement between molecules after aging, so the viscosity increased after aging at 150°C.

#### Tribological Properties of OBent

The tribological properties of the drilling muds were evaluated using a UMT-2 tribotester in ball-on-plate mode (Fig. 9). OBent showed a smaller wear rate and friction coefficient than raw bentonite. The friction coefficients of OBent did not show significant change as HDTMS increased (Fig. 9a). The friction coefficients of OBent were all smaller than that of CTAB-Bent, however. The wear rate and the two-dimensional graph of wear track (Fig. 9b,c) showed that HDTMS (1)-CTAB (0.5)-Bent/oil had the smallest wear rate and the best antiwear property. The main reason was that the compatibility between OBent and white oil increased when the amount of HDTMS increased, and an organic lubricating film was formed on the surface of the friction pairs (Wang et al. 2011); thereby reducing the friction coefficient and wear rate.



## CONCLUSIONS

During this research, a comprehensive study was performed on bentonite co-modified by CTAB and HDTMS, with the purpose of gaining more thermally stable organic bentonite as additives in oil-based drilling muds, compared with bentonite modified by CTAB or HDTMS alone. The two surfactants on bentonite exhibited good synergistic effects with CTAB entering the interlayer space of bentonite through ion exchange to enlarge the basal spacing, which promoted more HDTMS to enter the interlayer spaces, and the formation of covalent bonds at the surface of platelets. As a result, the stability and dispersibility of bentonite were improved. Furthermore, co-modified bentonite demonstrated relatively stable rheological properties before and after aging at 150°C, and excellent friction-reducing and antiwear properties. In addition, HDTMS (1)-CTAB (0.5)-Bent showed significant hydrophobic properties and gel volume, because of the increase in surfactant HDTMS in bentonite. Bentonite without intercalation by CTAB was modified directly by HDTMS, however, and performed less well because of ineffective intercalation into the interlayer space of bentonite. HDTMS (1)-CTAB (0.5)-Bent can potentially be used in oil-based drilling muds in drilling operations.

## ACKNOWLEDGMENTS

The authors acknowledge the financial support provided by National Natural Science Foundation of China (grant Nos. 51775168, 21671053, 51875172, 51605143, and 51605469), by the scientific and technological innovation team of Henan Province University (grant No. 19IRTSTHN024), Science and Technology Development Plan Project of Henan Province (202102210254), and Key Scientific Research Project of Colleges and Universities in Henan Province (20A150003)

## Funding

Funding sources are as stated in the Acknowledgments.

## Compliance with Ethical Standards

## Conflict of Interest

The authors declare that they have no conflict of interest.

## REFERENCES

- Asgari, M., Abouelmagd, A., & Sundararaj, U. (2017). Silane functionalization of sodium montmorillonite nanoclay and its effect on rheological and mechanical properties of HDPE/clay nanocomposites. *Applied Clay Science*, *146*, 439–448.
- Asgari, M., & Sundararaj, U. (2018a). Pre-exfoliated nanoclay through two consecutive reaction systems: Silane functionalization followed by grafting of amino acid monomers. *Applied Clay Science*, *151*, 81–91.
- Asgari, M., & Sundararaj, U. (2018b). Silane functionalization of sodium montmorillonite nanoclay: The effect of dispersing media on intercalation and chemical grafting. *Applied Clay Science*, *153*, 228–238.
- Awad, A. M., Shaikh, S. M. R., Jalab, R., Gulied, M. H., Nasser, M. S., Benamor, A., & Adham, S. (2019). Adsorption of organic pollutants by natural and modified clays: A comprehensive review. *Separation and Purification Technology*, *228*, 115719.
- Battas, A., Gaidoumi, A. E., Ksakas, A., & Kherbeche, A. (2019). Adsorption study for the removal of nitrate from water using local clay. *The Scientific World Journal*, *2019*, 9529618.
- Bergaya, F., & Lagaly, G. (2001). Surface modification of clay minerals. *Applied Clay Science*, *19*, 1–3.
- Bujdák, J. (2015). Effect of layer charge on the formation of polymer/layered silicate nanocomposites: Intercalation of polystyrene. *The Journal of Physical Chemistry C*, *119*, 12016–12022.
- Caenn, R., & Chillingar, G. V. (1996). Drilling fluids: State of the art. *Journal of Petroleum Science and Engineering*, *14*, 221–230.
- Chen, T. X., Yuan, Y., Zhao, Y. L., Rao, F., & Song, S. X. (2018). Effect of layer charges on exfoliation of montmorillonite in aqueous solutions. *Colloids and Surfaces A: Physicochemical and Engineering Aspects*, *548*, 92–97.
- de Paiva, L. B., Morales, A. R., & Valenzuela Díaz, F. R. (2008). Organoclays: Properties, preparation and applications. *Applied Clay Science*, *42*, 8–24.
- El Gaidoumi, A., Chaoui Benabdallah, A., El Bali, B., & Kherbeche, A. (2018). Synthesis and characterization of zeolite HS using natural pyrophyllite as new clay source. *Arabian Journal for Science and Engineering*, *43*, 191–197.
- El Gaidoumi, A., Dona-Rodriguez, J. M., Pulido Melian, E., Gonzalez-Diaz, O. M., Navio, J. A., El Bali, B., & Kherbeche, A. (2019a). Catalytic efficiency of Cu-supported pyrophyllite in heterogeneous catalytic oxidation of phenol. *Arabian Journal for Science and Engineering*, *44*, 6313–6325.
- El Gaidoumi, A., Loqman, A., Benadallah, A. C., El Bali, B., & Kherbeche, A. (2019b). Co (ii)-pyrophyllite as catalyst for phenol oxidative degradation: Optimization study using response surface methodology. *Waste and Biomass Valorization*, *10*, 1043–1051.
- El Gaidoumi, A., Miguel Dona-Rodriguez, J., Pulido Melian, E., Manuel Gonzalez-Diaz, O., El Bali, B., Antonio Navio, J., & Kherbeche, A. (2019c). Mesoporous pyrophyllite-titania nanocomposites: Synthesis and activity in phenol photocatalytic degradation. *Research on Chemical Intermediates*, *45*, 333–353.
- Erdem, B., Özcan, A. S., & Özcan, A. (2010). Preparation of hdtm-bentonite: Characterization studies and its adsorption behavior toward dibenzofuran. *Surface and Interface Analysis*, *42*, 1351–1356.
- Fu, M., Zhang, Z. P., Wu, L. M., Zhuang, G. Z., Zhang, S., Yuan, J. Y., & Liao, L. B. (2016). Investigation on the co-modification process of montmorillonite by anionic and cationic surfactants. *Applied Clay Science*, *132–133*, 694–701.
- Gamba, M., Kovář, P., Pospíšil, M., & Torres Sánchez, R. M. (2017). Insight into thiabendazole interaction with montmorillonite and organically modified montmorillonites. *Applied Clay Science*, *137*, 59–68.
- Geyer, B., Hundhammer, T., Röhner, S., Lorenz, G., & Kandelbauer, A. (2014). Predicting thermal and thermo-oxidative stability of silane-modified clay minerals using thermogravimetry and isoconversional kinetic analysis. *Applied Clay Science*, *101*, 253–259.
- He, H., Ding, Z., Zhu, J., Yuan, P., Xi, Y., Yang, D., & Frost, R. L. (2005). Thermal characterization of surfactant-modified montmorillonites. *Clays and Clay Minerals*, *53*, 287–293.
- He, H., Ma, L., Zhu, J., Frost, R. L., Theng, B. K. G., & Bergaya, F. (2014). Synthesis of organoclays: A critical review and some unresolved issues. *Applied Clay Science*, *100*, 22–28.
- Hunnicutt, M. L., & Harris, J. M. (1986). Reactivity of organosilane reagents on microparticulate silica. *Analytical Chemistry*, *58*, 748–752.
- Huskić, M., Žigon, M., & Ivanković, M. (2013). Comparison of the properties of clay polymer nanocomposites prepared by montmorillonite modified by silane and by quaternary ammonium salts. *Applied Clay Science*, *85*, 109–115.

- Impens, N. R. E., van der Voort, P., & Vansant, E. F. (1999). Silylation of micro-, meso- and non-porous oxides: A review. *Microporous and Mesoporous Materials*, 28, 217–232.
- Kaufhold, S., & Dohrmann, R. (2013). The variable charge of dioctahedral smectites. *Journal of Colloid and Interface Science*, 390, 225–233.
- Meng, X. H., Zhang, Y. H., Zhou, F. S., & Chu, P. K. (2012). Effects of carbon ash on rheological properties of water-based drilling fluids. *Journal of Petroleum Science and Engineering*, 100, 1–8.
- Minase, M., Kondo, M., Onikata, M., & Kawamura, K. (2008). The viscosity of organic liquid suspensions of trimethyldecylammonium-montmorillonite complexes. *Clays and Clay Minerals*, 56, 49–65.
- Mustapha, S., Ndamitso, M. M., Abdulkareem, A. S., Tijani, J. O., Shuaib, D. T., Ajala, A. O., & Mohammed, A. K. (2020). Application of TiO<sub>2</sub> and ZnO nanoparticles immobilized on clay in wastewater treatment: A review. *Applied Water Science*, 10, 1–36.
- Pavlidou, S., & Papispyrides, C. D. (2008). A review on polymer-layered silicate nanocomposites. *Progress in Polymer Science*, 33, 1119–1198.
- Piscitelli, F., Posocco, P., Toth, R., Fermeglia, M., Pricl, S., Mensitieri, G., & Lavorgna, M. (2010). Sodium montmorillonite silylation: Unexpected effect of the aminosilane chain length. *Journal of Colloid and Interface Science*, 351, 108–115.
- Raji, M., Mekhzoum, M. E. M., Rodrigue, D., Qaiss, A. E. K., & Bouhfid, R. (2018). Effect of silane functionalization on properties of polypropylene/clay nanocomposites. *Composites Part B: Engineering*, 146, 106–115.
- Shanmugharaj, A. M., Rhee, K. Y., & Ryu, S. H. (2006). Influence of dispersing medium on grafting of aminopropyltriethoxysilane in swelling clay materials. *Journal of Colloid and Interface Science*, 298, 854–859.
- Shen, T., & Gao, M. (2019). Gemini surfactant modified organo-clays for removal of organic pollutants from water: A review. *Chemical Engineering Journal*, 375, 1–27.
- Shen, H., Lv, K., Huang, X., Liu, J., Bai, Y., Wang, J., & Sun, J. (2019). Hydrophobic-associated polymer-based laponite nanolayered silicate composite as filtrate reducer for water-based drilling fluid at high temperature. *Journal of Applied Polymer Science*, 137, 48608.
- Sinha Ray, S., & Okamoto, M. (2003). Polymer/layered silicate nanocomposites: A review from preparation to processing. *Progress in Polymer Science*, 28, 1539–1641.
- Song, K. (2001). Characterization of montmorillonite surfaces after modification by organosilane. *Clays and Clay Minerals*, 49, 119–125.
- Sun, J. L., Zhuang, G. Z., Wu, S. Q., & Zhang, Z. P. (2016). Structure and performance of anionic-cationic-organo-montmorillonite in different organic solvents. *RSC Advances*, 6, 54747–54753.
- van Olphen, H. (1964). Internal mutual flocculation in clay suspensions. *Journal of Colloid Science*, 19, 313–322.
- Waddell, T. G., Leyden, D. E., & DeBello, M. T. (1981). The nature of organosilane to silica-surface bonding. *Journal of the American Chemical Society*, 103, 5303–5307.
- Wang, Z. Y., Xia, Y. Q., & Liu, Z. L. (2011). Study the sensitivity of solid lubricating additives to attapulgite clay base grease. *Tribology Letters*, 42, 141–148.
- Xi, Y. F., Zhou, Q., Frost, R. L., & He, H. P. (2007). Thermal stability of octadecyltrimethylammonium bromide modified montmorillonite organoclay. *Journal of Colloid and Interface Science*, 311, 347–353.
- Xie, W., Gao, Z. M., Pan, W. P., Hunter, D., Singh, A., & Vaia, R. (2001). Thermal degradation chemistry of alkyl quaternary ammonium montmorillonite. *Chemistry of Materials*, 13, 2979–2990.
- Yang, Y., Zhu, Z. K., Yin, J., Wang, X. Y., & Qi, Z. E. (1999). Preparation and properties of hybrids of organo-soluble polyimide and montmorillonite with various chemical surface modification methods. *Polymer*, 40, 4407–4414.
- Zhong, Y., & Wang, S. Q. (2003). Exfoliation and yield behavior in nanodispersions of organically modified montmorillonite clay. *Journal of Rheology*, 47, 483–495.
- Zhu, L. Z., Tian, S. L., Zhu, J. X., & Shi, Y. (2007). Silylated pillared clay (SPILC): A novel bentonite-based inorgano-organo composite sorbent synthesized by integration of pillaring and silylation. *Journal of Colloid and Interface Science*, 315, 191–199.
- Zhuang, G. Z., Zhang, Z. P., Fu, M., Ye, X., & Liao, L. B. (2015). Comparative study on the use of cationic-nonionic-organo-montmorillonite in oil-based drilling fluids. *Applied Clay Science*, 116–117, 257–262.
- Zhuang, G. Z., Zhang, Z. P., Sun, J. L., & Liao, L. B. (2016). The structure and rheology of organo-montmorillonite in oil-based system aged under different temperatures. *Applied Clay Science*, 124–125, 21–30.
- Zhuang, G. Z., Zhang, H. X., Wu, H., Zhang, Z. P., & Liao, L. B. (2017a). Influence of the surfactants' nature on the structure and rheology of organo-montmorillonite in oil-based drilling fluids. *Applied Clay Science*, 135, 244–252.
- Zhuang, G. Z., Zhang, Z. P., Wu, H., Zhang, H. X., Zhang, X. M., & Liao, L. B. (2017b). Influence of the nonionic surfactants' nature on the structures and properties of organo-montmorillonites. *Colloids and Surfaces A: Physicochemical and Engineering Aspects*, 518, 116–123.
- Zhuang, G. Z., Zhang, Z. P., Peng, S. M., Gao, J. H., Pereira, F. A. R., & Jaber, M. (2019). The interaction between surfactants and montmorillonite and its influence on the properties of organo-montmorillonite in oil-based drilling fluids. *Clays and Clay Minerals*, 67, 190–208.

(Received 1 May 2020; revised 23 July 2020; AE: Jun Kawamata)